

# Theoretical (DFT) Insights into the Mechanism of Copper-Catalyzed Cyclopropanation Reactions. Implications for Enantioselective Catalysis

José M. Fraile,<sup>‡</sup> José I. García,<sup>\*,‡</sup> Víctor Martínez-Merino,<sup>†</sup> José A. Mayoral,<sup>‡</sup> and Luis Salvatella<sup>\*,‡</sup>

Contribution from the Departamento de Química Orgánica, Instituto de Ciencia de Materiales de Aragón, C.S.I.C.-Universidad de Zaragoza, Pedro Cerbuna 12, E-50009 Zaragoza, Spain, and the Departamento de Química Aplicada, Universidad Pública de Navarra, E-31006 Pamplona, Spain

Received October 16, 2000. Revised Manuscript Received June 4, 2001

**Abstract:** The mechanism of the copper(I)-catalyzed cyclopropanation reaction has been extensively investigated for a medium-size reaction model by means of B3LYP/6-31G(d) calculations. The starting ethylene complex of the *N,N'*-dimethylmalonaldiimine–copper (I) catalyst undergoes a ligand exchange with methyl diazoacetate to yield a reaction intermediate, which subsequently undergoes nitrogen extrusion to generate a copper–carbene complex. The cyclopropanation step takes place through a direct carbene insertion of the metal–carbene species to yield a catalyst–product complex, which can finally regenerate the starting complex. The stereochemical predictions of a more realistic model (by considering a chiral bis(oxazoline)–copper (I) catalyst) have been rationalized in terms of steric repulsions, showing good agreement with experimental data.

## Introduction

Cyclopropane derivatives are an important family of chemical compounds due to their interesting biological properties<sup>1</sup> as well as their use as starting materials and intermediates in organic synthesis.<sup>2</sup> As a result, great efforts have been made to develop efficient diastereo- and enantioselective methods for the synthesis of cyclopropanes.<sup>3</sup> A particularly versatile method is the metal-catalyzed cyclopropanation of olefins with diazo compounds, for which various efficient homogeneous catalysts have been developed.

The use of catalysts based on copper is particularly attractive because of their high efficiency in asymmetric cyclopropanation reactions<sup>4</sup> and their relatively low cost in comparison with other metal derivatives, such as catalysts based on rhodium<sup>5</sup> or ruthenium.<sup>6</sup> In fact, the asymmetric cyclopropanation of styrene with diazo esters, catalyzed by chiral copper salicylaldehyde complexes, was reported in 1966 as the first example of an enantioselective reaction under homogeneous catalytic conditions.<sup>7</sup> Since then, other chiral ligands, such as chiral salicyl-

aldehyde–amino acid derivatives<sup>8</sup> or semicorrins,<sup>9</sup> have been used in copper-catalyzed asymmetric cyclopropanation reactions. Among them, the best results have been obtained with bis(oxazolines), independently described by the groups of Evans<sup>10</sup> and Masamune,<sup>11</sup> which can lead to almost complete enantioselectivity (up to 99% ee) when their complexes with Cu(I) or Cu(II) are used in cyclopropanation reactions. The good performance of chiral bis(oxazolines) as ligands for asymmetric cyclopropanation, as well as for other Lewis acid-catalyzed reactions, has resulted in the recent commercial availability of a number of these compounds.

From the point of view of large-scale applications, the ease of use and recovery of the chiral catalysts have become important and several studies have been published that focus on the immobilization of this kind of catalyst.<sup>12,13</sup>

In both the homogeneous and heterogeneous phases, the dependence of the stereoselectivity on factors such as the solvent, the counterion, or the structure of the chiral ligand has been described.<sup>13,14</sup> However, the mechanism of the copper-catalyzed cyclopropanation reactions of diazo compounds has remained controversial even for the nonchiral systems. A deeper

<sup>‡</sup> C.S.I.C.-Universidad de Zaragoza.

<sup>†</sup> Universidad Pública de Navarra.

(1) Suckling, C. J. *Angew. Chem., Int. Ed. Engl.* **1988**, *27*, 537–552.

(2) Wong, H. N. C.; Hon, M.-Y.; Tse, C.-W.; Yip, Y.-C.; Tanko, J.; Hudlicky, T. *Chem. Rev.* **1989**, *89*, 165–198.

(3) (a) Ye, T.; McKervey, M. A. *Chem. Rev.* **1994**, *94*, 1091–1160. (b) Singh, V. K.; Gupta, A. D.; Sekar, G. *Synthesis* **1997**, 137–149. (c) Doyle, M. P.; Protopopova, M. N. *Tetrahedron* **1998**, *54*, 7919–7946.

(4) Pfaltz, A. Cyclopropanation and C–H Insertion with Cu. In *Comprehensive Asymmetric Catalysis*; Jacobsen, E. N., Pfaltz, A., Yamamoto, H., Eds.; Springer-Verlag: Berlin, 1999; Vol. 2, pp 513–538.

(5) Lydon, K. M.; McKervey, M. A. Cyclopropanation and C–H Insertion with Rh. In *Comprehensive Asymmetric Catalysis*; Jacobsen, E. N., Pfaltz, A., Yamamoto, H., Eds.; Springer-Verlag: Berlin, 1999; Vol. 2, pp 539–580.

(6) Charette, A. B.; Lebel, H. Cyclopropanation and C–H Insertion with Metals other than Cu and Rh. In *Comprehensive Asymmetric Catalysis*; Jacobsen, E. N., Pfaltz, A., Yamamoto, H., Eds.; Springer-Verlag: Berlin, 1999; Vol. 2, pp 581–603.

(7) Nozaki, H.; Moriuti, S.; Takaya, H.; Noyori, R. *Tetrahedron Lett.* **1966**, 5239–5244.

(8) Aratani, T. *Pure Appl. Chem.* **1985**, *57*, 1839–1844.

(9) Leutenegger, U.; Umbricht, G.; Fahrni, C.; Matt, P.; Pfaltz, A. *Tetrahedron* **1992**, *48*, 2143–2156.

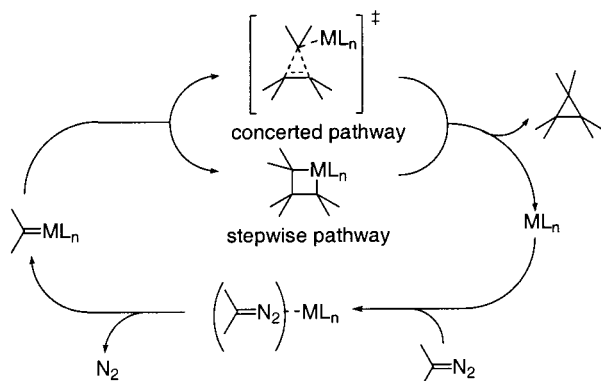
(10) Evans, D. A.; Woerpel, K. A.; Hinman, M. M.; Faul, M. M. *J. Am. Chem. Soc.* **1991**, *113*, 726–728.

(11) Lowenthal, R. E.; Abiko, A.; Masamune, T. *Tetrahedron Lett.* **1990**, *31*, 6005–6008.

(12) (a) Fraile, J. M.; García, J. I.; Mayoral, J. A.; Tarnai, T. *Tetrahedron: Asymmetry* **1998**, *9*, 3997–4008. (b) Fraile, J. M.; García, J. I.; Mayoral, J. A.; Tarnai, T.; Harmer, M. A. *J. Catal.* **1999**, *186*, 214–221.

(13) Díaz-Requejo, M. M.; Nicasio, M. C.; Pérez, P. J. *Organometallics* **1998**, *17*, 3051–3057.

(14) (a) Fraile, J. M.; García, J. I.; Mayoral, J. A.; Tarnai, T. *J. Mol. Catal. A* **1999**, *144*, 85–89. (b) Llewellyn, D. B.; Adamson, D.; Arndtsen, B. A. *Org. Lett.* **2000**, *2*, 4165–4168.

**Scheme 1.** Possible Catalytic Cycles for Metal-Catalyzed Cyclopropanation Reactions

understanding of this mechanism would undoubtedly lead to the design of even better catalysts.

Some aspects of the reaction mechanism are clear. The oxidation state of the copper center in the active catalyst is one point that must be considered. It has been observed that Cu(II) complexes are reduced to Cu(I) derivatives by the diazo compound under the reaction conditions.<sup>15</sup> This has led to general agreement that the active catalyst is a Cu(I) species, irrespective of the oxidation state of the copper complex used as the precatalyst.<sup>8,15,16</sup>

It is also generally accepted that transition metal-catalyzed cyclopropanation reactions proceeds via a metal-carbene complex, which is formed by association of the diazo compound and the catalyst with concomitant extrusion of nitrogen. However, the details of this process are not well-known.<sup>17</sup> Only very recently copper-carbene complexes have been detected as reaction intermediates in cyclopropanation reactions.<sup>18</sup> Other metal-carbene derivatives, such as systems containing ruthenium or osmium, had previously been isolated from stoichiometric reactions with diazo esters and have proven to be active catalysts in these processes.<sup>19</sup>

It has been shown that the formation of the copper-carbene intermediate is the rate-limiting step of the cyclopropanation reaction.<sup>15,20</sup> However, given that the carbene insertion occurs after this step, only the stereochemical product distribution can offer some mechanistic insight.<sup>21</sup> A detailed knowledge of the step that controls the stereochemistry of the reaction products is clearly indispensable for the rational design of new enantioselective catalysts.

Two different mechanisms for the copper-catalyzed formation of the cyclopropane ring have been proposed (Scheme 1),<sup>22</sup> namely the concerted pathway (henceforth referred to as direct carbene insertion)<sup>16,23</sup> and a two-step process that proceeds via a metallacyclobutane intermediate.<sup>8,24</sup> This alternative is well

(15) Salomon, R. G.; Kochi, J. K. *J. Am. Chem. Soc.* **1973**, *95*, 3300–3310.

(16) Fritschi, H.; Leutenegger, U.; Pfaltz, A. *Helv. Chim. Acta* **1988**, *71*, 1553–1565.

(17) Doyle, M. P. Transition Metal Carbene Complexes: Diazodecomposition, Ylide, and Insertion. In *Comprehensive Organometallic Chemistry II*; Abel, E. W., Stone, F. G. A., Wilkinson, G., Eds.; Pergamon: Oxford, 1995; Vol. 12, pp 421–468.

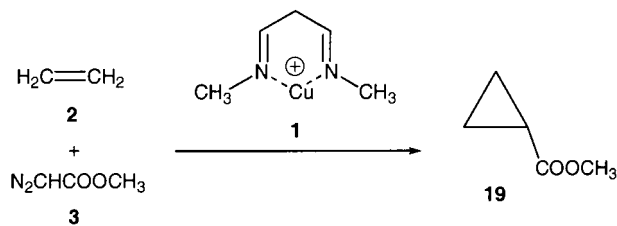
(18) Straub, B. F.; Hofmann, P. *Angew. Chem., Int. Ed. Engl.* **2001**, *40*, 1288–1290.

(19) (a) Smith, D. A.; Reynolds, D. N.; Woo, L. K. *J. Am. Chem. Soc.* **1993**, *115*, 2511–2513. (b) Collman, J. P.; Rose, E.; Venburg, G. D. *J. Chem. Soc., Chem. Commun.* **1993**, 934–935. (c) Park, S.-B.; Sakata, N.; Nishiyama, H. *Chem. Eur. J.* **1996**, *2*, 303–306.

(20) Díaz-Requejo, M. M.; Belderrain, T. R.; Nicasio, M. C.; Prieto, F.; Pérez, P. J. *Organometallics* **1999**, *18*, 2601–2609.

(21) Moser, W. R. *J. Am. Chem. Soc.* **1969**, *91*, 1135–1140.

(22) Brookhart, M.; Studabaker, W. B. *Chem. Rev.* **1987**, *87*, 411–432.

**Scheme 2.** Model Cu-Catalyzed Cyclopropanation Reaction

illustrated by the different mechanistic behavior found for compounds based on two species that are isoelectronic to the copper(I) cation, namely the zinc(II) ion and the nickel(0) atom. Thus, Simmons–Smith cyclopropanation of zinc carbenoid species takes place through a direct carbene insertion.<sup>25</sup> Instead, nickel(0) carbene complexes react with olefins to yield metal-lacyclobutanes, which can subsequently generate cyclopropanes by reductive elimination.<sup>26</sup>

A detailed mechanistic study of the copper-catalyzed cyclopropanation, including the nature of short-lived species and transition states, can be carried out by means of theoretical calculations. In this paper we present a study of the mechanism of a copper-catalyzed cyclopropanation reaction on a medium-size reaction model by means of a theoretical approach based on the Density Functional Theory (DFT). Furthermore, the different approximations between the reactants in the step controlling the stereochemistry of the cyclopropanation process have been studied by considering a chiral bis(oxazoline) as a more realistic catalyst model for the reactions of unsubstituted (ethylene) and substituted (propene) olefins.

A more restricted study for different reaction models has been independently achieved by Norrby and co-workers,<sup>27</sup> in which no transition states could be characterized. A recent study of the copper-catalyzed aziridination reaction mechanistically related to the cyclopropanation process was also carried out by the same research group.<sup>28</sup>

## Methods

A comprehensive mechanistic study of the copper-catalyzed cyclopropanation reaction was carried out by means of a medium-size model including a number of simple reactants considered in this study: *N,N'*-dimethylmalonaldimine–copper(I) cation (denoted as **1**) as the catalyst, ethylene (**2**) as the olefin, and methyl diazoacetate (**3**) as the diazo compound (Scheme 2). The formation of the copper-carbene complex and two alternative pathways for the cyclopropanation reaction (direct carbene insertion and two-step mechanism) were studied in this work.

(23) (a) Moser, W. R. *J. Am. Chem. Soc.* **1969**, *91*, 1141–1146. (b) Gupta, A. D.; Bhuniya, D.; Singh, V. K. *Tetrahedron* **1994**, *50*, 13725–13730. (c) Gant, T. G.; Noe, M. C.; Corey, E. J. *Tetrahedron Lett.* **1995**, *36*, 8745–8748. (d) Doyle, M. P., Ed. *Advances in Catalytic Processes*; Jai Press: London, 1995; Vol. 1, p 69. (e) Kwong, H.-L.; Lee, W.-S. *Tetrahedron: Asymmetry* **2000**, *11*, 2299–2308.

(24) (a) Noyori, R. *Asymmetric Catalysis in Organic Synthesis*; Wiley: New York, 1994. (b) Ichianagi, T.; Shimizu, M.; Fujisawa, T. *Tetrahedron* **1997**, *53*, 9599–9610. (c) Cho, D.-J.; Jeon, S.-J.; Kim, H.-S.; Cho, C.-S.; Shim, S.-C.; Kim, T.-J. *Tetrahedron: Asymmetry* **1999**, *10*, 3833–3848. (d) Li, Z.; Liu, G.; Zheng, Z.; Chen, H. *Tetrahedron* **2000**, *56*, 7187–7191.



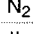
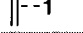
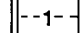
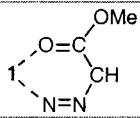
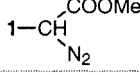
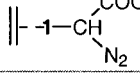
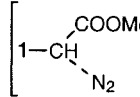
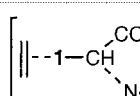
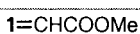
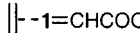
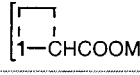

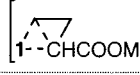
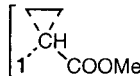
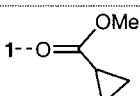
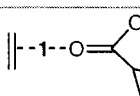

(25) (a) Dargel, T. K.; Koch, W. *J. Chem. Soc., Perkin Trans. 2* **1996**, 877–881. (b) Bernardi, F.; Bottoni, A.; Miscione, G. P. *J. Am. Chem. Soc.* **1997**, *119*, 12300–12305. (c) Hirai, A.; Nakamura, M.; Nakamura, E. *Chem. Lett.* **1998**, 927–928. (d) Bernardi, F.; Bottoni, A.; Miscione, G. P. *Organometallics* **2000**, *19*, 5529–5532.

(26) (a) Jennings, P. W.; Johnson, L. L. *Chem. Rev.* **1994**, *94*, 2241–2291. (b) Cámpora, J.; Palma, P.; Carmona, E. *Coord. Chem. Rev.* **1999**, *193–195*, 207–281.

(27) Rasmussen, T.; Jensen, J. F.; Ziegler, T.; Norrby, P.-O. Manuscript submitted for publication.

(28) Brandt, P.; Södergren, M. J.; Andersson, P. G.; Norrby, P.-O. *J. Am. Chem. Soc.* **2000**, *122*, 8013–8020.

**Table 1.** Numbering and Relative Gibbs Free Energies (kcal mol<sup>-1</sup>) of the Different Structures Considered in This Work

Schematic Picture	Structure Number	Relative Energy
<b>1</b>	<b>1</b>	0
	<b>2</b>	0
	<b>3</b>	0
	<b>4</b>	0
	<b>5</b>	-34.2
	<b>6</b>	-27.3
	<b>7</b> chelate complex	-32.6
	<b>7</b>	-20.9
	<b>8</b>	-27.7
	<b>9</b>	-13.0
	<b>10</b>	-10.5
	<b>11</b>	-35.2
	<b>12</b>	-29.5
	<b>13</b>	-22.4
	<b>14</b>	-65.8
	<b>15</b>	-63.5
	<b>16</b>	-25.3
	<b>17</b>	-78.1
	<b>18</b>	-90.4
	<b>19</b>	-51.9

It should be noted that a bidentate ligand-copper(I) complex has two vacant coordination sites. Whereas one of these coordination sites is certainly involved in the catalysis of the cyclopropanation reaction, the role of the other vacant site is less clear. It is possible that this site could be occupied by the negative counterion, but it is well-known that the best performance for this kind of catalyst is achieved with weakly coordinating anions such as triflate. Furthermore, the solvents usually used in cyclopropanation reactions are also poorly coordinating. Thus, two concurrent mechanisms can be considered depending on the possibility of coordination of an additional olefin molecule to the metal, as suggested for a rhodium-catalyzed cyclopropanation reaction.<sup>29</sup> Therefore, the possible involvement of an ethylene molecule has also been considered throughout this work. The possibility of different

conformations was taken into account for all structures, although the discussion of the results is centered on the most stable form in each case.

All calculations were carried out by means of the B3LYP hybrid functional<sup>30</sup> because of the satisfactory performance of this technique in the chemistry of transition metals.<sup>31</sup> In particular, excellent results are found for Cu(I) binding energies of methylene as well as some nitrogen ligands.<sup>32</sup> Full optimizations using the 6-31G(d) basis set for all the atoms were carried out using the Gaussian 98 package.<sup>33</sup> No BSSE corrections have been considered throughout this work.

Analytical frequencies were calculated at the B3LYP/6-31G(d) level and the nature of the stationary points was determined in each case according to the right number of negative eigenvalues of the Hessian matrix. Scaled frequencies were not considered since significant errors on the calculated thermodynamical properties are not found at this theoretical level.<sup>34</sup>

In the case of the chiral models, single-point energy calculations at the B3LYP/6-311+G(2d,p) level were carried out on the B3LYP/6-31G(d) geometries. Furthermore, solvent effects were taken into account through the IPCM method,<sup>35</sup> as implemented in Gaussian 98. The dielectric permittivity of dichloromethane ( $\epsilon = 8.93$ ) was used, together with an isodensity cutoff value of 0.0001.

Unless otherwise stated, only Gibbs free energies are used for the discussion on the relative stabilities of the chemical structures considered. Relative free energies (including thermal corrections at 25 °C) of the structures considered are shown in Table 1. Hard data on electronic energies, as well as entropies, enthalpies, Gibbs free energies, and lowest frequencies of the different conformations of all structures considered, are available as Supporting Information.

## Results and Discussion

**Formation of the Copper-Carbene Complex.** The structures of the catalyst and reactants considered in this work are shown in Figure 1. The catalyst (**1**) has a planar framework with the copper in a bent coordination with Cu...N distances of 1.840 Å. Ethylene (**2**) also has a planar structure, as one would expect. On the other hand, both *s-cis* and *s-trans* conformers are possible for methyl diazoacetate (**3**) depending on the relative position of the dinitrogen and carbonyl groups around the C-C bond. Free energy calculations indicate that the *s-cis* conformer is very slightly favored according to free energy calculations (by 0.01 kcal mol<sup>-1</sup>), in agreement with experimental data, which shows the same preference by 0.07 kcal mol<sup>-1</sup>.<sup>36</sup> Since dinitrogen (**4**) is a byproduct of the cyclopropanation, the corresponding structure was studied and gave a diatomic molecule with a bond length of 1.106 Å.

An energy diagram for the catalytic cycle is displayed in Figure 2, with the favored mechanism represented by solid lines

(29) Maxwell, J. L.; Brown, K. C.; Bartley, D. W.; Kodadek, T. *Science* **1992**, *256*, 1544-1547.

(30) (a) Lee, C.; Yang, W.; Parr, R. *Phys. Rev. B* **1988**, *37*, 785-789. (b) Becke, A. D. *J. Chem. Phys.* **1993**, *98*, 5648-5652.

(31) Niu, S.; Hall, M. B. *Chem. Rev.* **2000**, *100*, 353-406.

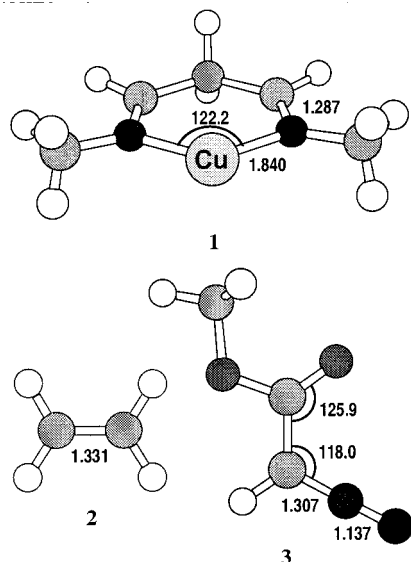
(32) Luna, A.; Alcamí, M.; M6, O.; Yáñez, M. *Chem. Phys. Lett.* **2000**, *320*, 129-138.

(33) Frisch, M. J.; Trucks, G. W.; Schlegel, H. B.; Scuseria, G. E.; Robb, M. A.; Cheeseman, J. R.; Zakrzewski, V. G.; Montgomery, J. A., Jr.; Stratmann, R. E.; Burant, J. C.; Dapprich, S.; Millan, J. M.; Daniels, A. D.; Kudin, K. N.; Strain, M. C.; Farkas, O.; Tomasi, J.; Barone, V.; Cossi, M.; Cammi, R.; Mennucci, B.; Pomelli, C.; Adamo, C.; Clifford, S.; Ochterski, J.; Petersson, G. A.; Ayala, P. Y.; Cui, Q.; Morokuma, K.; Malick, D. K.; Rabuck, A. D.; Raghavachari, K.; Foresman, J. B.; Cioslowski, J.; Ortiz, J. V.; Stefanov, B. B.; Liu, G.; Liashenko, A.; Piskorz, P.; Komaroni, I.; Gomperts, R.; Martin, R. L.; Fox, D. J.; Keith, T.; Al-Laham, M. A.; Peng, C. Y.; Nanayakkara, A.; González, C.; Challacombe, M.; Gill, P. M. W.; Johnson, B.; Chen, W.; Replogle, E. S.; Pople, J. A. *Gaussian98*, Revision A.7; Gaussian, Inc.: Pittsburgh, PA, 1998.

(34) Bauschlicher, C. W., Jr. *Chem. Phys. Lett.* **1995**, *246*, 40-44.

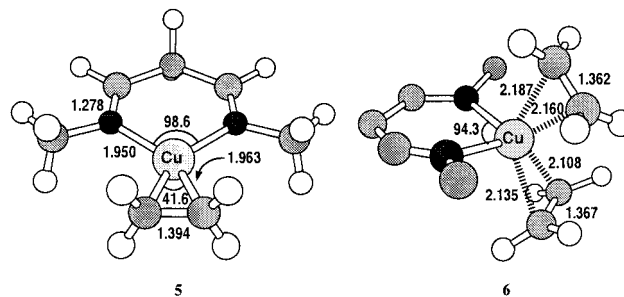
(35) Foresman, J. B.; Keith, T. A.; Wiberg, K. B.; Snoonian, J.; Frisch, M. J. *J. Phys. Chem.* **1996**, *100*, 16098-16104.

(36) Kaplan, F.; Meloy, G. K. *J. Am. Chem. Soc.* **1966**, *88*, 950-956.



**Figure 1.** Structures of the catalyst (1), ethylene (2), and methyl diazoacetate (3).

and the alternative pathways by hashed lines. The relative free energies of the structures shown in the diagram (in kcal mol<sup>-1</sup>) take into account the evolution of the system composition according to the different molecules entering or leaving the system. As shown in Table 1, the catalyst (1), ethylene (2), methyl diazoacetate (3), and dinitrogen (4) have been arbitrarily chosen as reference points for the calculation of relative free

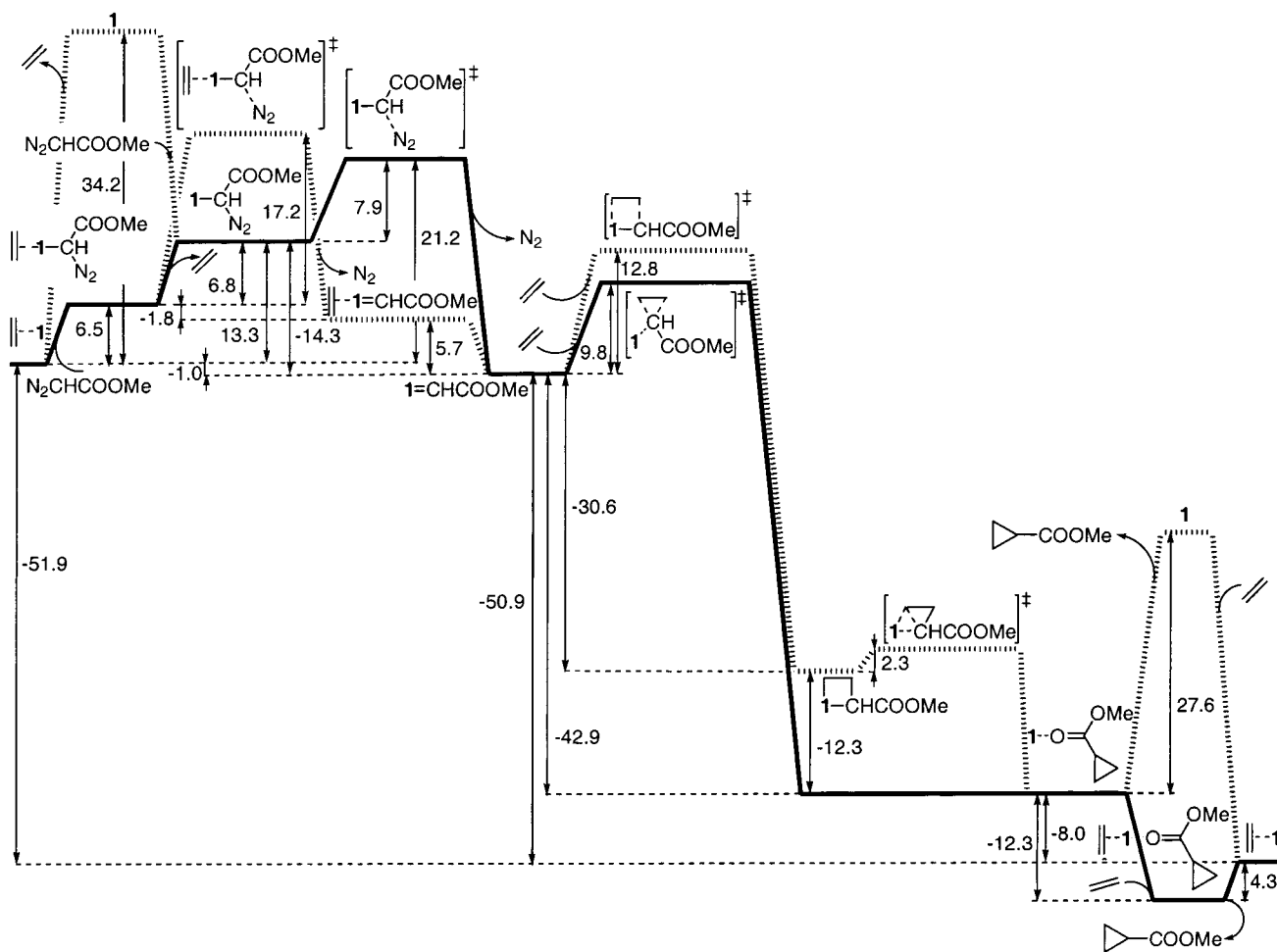


**Figure 3.** Structures of both 1:1 (5) and 1:2 (6) catalyst-ethylene complexes (some hydrogen atoms have been omitted for clarity).

energies. As a consequence of the choice of this reference framework, the catalyst-ethylene complex shown on the right of the diagram is more stable than that situated on the left since the free energy of the overall cyclopropanation reaction is implicitly included there. The sign criterion of the relative free energy corresponds to the variation in the direction from left to right (according to the diagram).

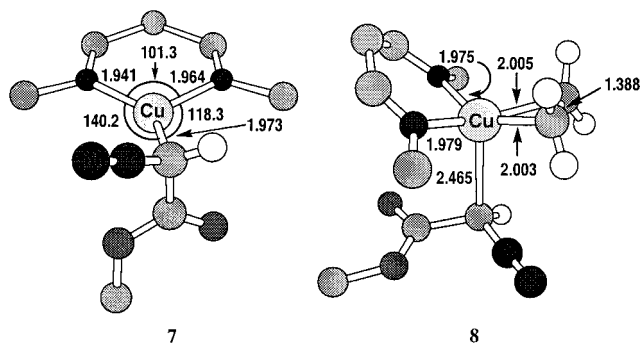
Kinetic studies have shown that olefin excess slows down the rate of cyclopropanation and this result is attributed to the existence of a preequilibrium involving the formation of catalyst-olefin complexes.<sup>13,15,20</sup> The stoichiometry of such species in the reaction conditions makes this a significant point.<sup>13,20,23</sup>

The structures of the catalyst-olefin complexes with 1:1 (denoted as 5) and 1:2 (6) stoichiometries are shown in Figure 3. The structure of 5 presents a trigonal coordination for copper



**Figure 2.** Energy diagram for a catalytic cycle.





**Figure 4.** Nonassisted (**7**) and olefin-assisted (**8**) structures of the catalyst–diazo ester complexes (some hydrogen atoms have been omitted for clarity).

in such a way that carbon atoms are symmetrically located in the plane containing the catalyst framework, a situation in agreement with experimental data for other ethylene–copper(I) complexes.<sup>37</sup> The calculated Cu···C distance of 1.963 Å is also in good agreement with the experimental values found for these kinds of complexes (1.969–2.019 Å).<sup>37</sup> These structural results indicate the presence of a strong binding interaction for the catalyst–olefin complex.

On the other hand, the structure of **6** presents a tetrahedral copper atom coordinated to the two olefin molecules in agreement with experimental data for other copper–olefin complexes.<sup>38</sup> Energy results indicate that the formation of both **5** and **6** from the reactants is favored from a thermodynamical viewpoint (−34.2 and −27.3 kcal mol<sup>−1</sup>, respectively). These data indicate a preference for the 1:1 complex even in the presence of olefin excess, which is in agreement with experimental results obtained for other copper(I) complexes.<sup>39,40</sup> As a consequence, **5** is considered as the starting structure for a catalytic cycle.

A number of structures are conceivable for the catalyst–methyl diazoacetate coordination complex. Among them, the most stable species corresponds to a chelate in which copper is bound to both carbonyl oxygen and terminal diazo nitrogen atoms (not shown), in agreement with both theoretical and experimental data of related copper(I) complexes of diazo carbonyl compounds.<sup>41</sup> However, this structure has been excluded from the reaction diagram since a carbon–copper bond is required in it to allow the formation of the catalyst–carbene intermediate in a subsequent step, and therefore it represents a dead end in the reaction pathway.

Such a feature is found in a structure that is denoted as **7** in Figure 4. This structure is similar to theoretical calculations of a copper(I) complex of diazoacetaldehyde.<sup>41</sup> Furthermore, the occurrence of a metal–carbon bond in the catalyst–diazo ester complex is in accordance with the nature of the reaction intermediate detected in a rhodium-catalyzed cyclopropanation.<sup>29</sup> It can be remarked that the formation of the metal–carbon bond

involves the formal oxidation of copper(I) to copper(III). The Cu–C bond has a length of 1.973 Å, in agreement with experimental data for other copper(III) organometallic compounds (1.863–2.026 Å).<sup>42</sup> The binding energy between the catalyst and methyl diazoacetate (−20.9 kcal mol<sup>−1</sup>) is significantly lower than that calculated for ethylene complexation, and this finding is consistent with the behavior of Cu(I) ion as a soft Lewis acid.<sup>43</sup>

Three different reaction mechanisms can be considered, in principle, for the transformation of the catalyst–ethylene complex into the catalyst–diazo compound species, and these mechanisms are dissociative, associative, and interchange displacement.<sup>44</sup> The study of the catalyst–diazo ester interactions indicates that only the dissociative and associative mechanisms are possible for this ligand exchange.

The dissociative mechanism involves the formation of the naked catalyst, which can subsequently coordinate the diazo compound. Calculations indicate that the regeneration of the free catalyst requires a quite high energy (34.2 kcal mol<sup>−1</sup>), although this finding is contrary to experimental data that indicate copper-catalyzed cyclopropanation reactions to be relatively fast. Furthermore, a major role for the dissociative mechanism can be disregarded on the basis of experimental data indicating that ligand exchange of Cu(I)–olefin complexes requires the presence of coordinating impurities.<sup>39</sup>

Associative displacement is very common in the ligand exchange reactions of 16-electron complexes.<sup>45</sup> The exchange of ethylene by the diazo ester requires an energy increase of 12.0 kcal mol<sup>−1</sup>, a value derived from the different stability of the complexes involved. Although several ethylene–catalyst–methyl diazoacetate complexes are conceivable, a possible mechanism takes place through the structures denoted as **8**, having an intermediate energy between those of the complexes linking with each of the ligands since additional energy in the form of an activation barrier is not necessary. The catalyst–diazo compound complex can extrude dinitrogen to yield a copper–carbene complex through a transition state (denoted as **9**, Figure 5). The activation barrier for this elementary step is quite low (7.9 kcal mol<sup>−1</sup>) but the activation parameters for the overall process (i.e., from the starting compounds of the catalytic cycle) show moderate values ( $\Delta H_{298}^\ddagger = 21.5$  kcal mol<sup>−1</sup>,  $\Delta S_{298}^\ddagger = 0.7$  cal mol<sup>−1</sup> K<sup>−1</sup>,  $\Delta G_{298}^\ddagger = 21.2$  kcal mol<sup>−1</sup>). It can be seen in Figure 2 that this is the rate-limiting step of the reaction, which is in agreement with experimental data.<sup>15,20</sup>

The olefin-assisted mechanism for the formation of the catalyst–carbene complex can also be considered, the most stable transition structure (denoted as **10**) being shown in Figure 5. The copper–olefinic carbon bond lengths (2.081–2.101 Å) of the transition structure indicate a strong metal–alkene interaction. However, this pathway is disfavored by 2.5 kcal mol<sup>−1</sup> in comparison with the nonassisted mechanism. The preference for the nonassisted pathway agrees with experimental

(37) (a) Thompson, J. S.; Whitney, J. F. *Inorg. Chem.* **1984**, *23*, 2813–2819. (b) Masuda, H.; Yamamoto, N.; Taga, T.; Machida, K.; Kitagawa, S.; Munakata, M. *J. Organomet. Chem.* **1987**, *322*, 121–129. (c) Suenaga, Y.; Wu, L. P.; Kuroda-Sowa, T.; Munakata, M.; Maekawa, M. *Polyhedron* **1997**, *16*, 67–70.

(38) (a) Nickel, T.; Pörschke, K.-R.; Goddard, R.; Krüger, C. *Inorg. Chem.* **1992**, *31*, 4428–4430. (b) Olijnyk, V.; Glowiak, T.; Mys'kiv, M. *J. Chem. Crystallogr.* **1995**, *25*, 621–624.

(39) Cavallo, L.; Cucciolito, M. E.; De Martino, A.; Giordano, F.; Orabona, I.; Vitagliano, A. *Chem. Eur. J.* **2000**, *6*, 1127–1139.

(40) Munakata, M.; Kitagawa, S.; Shimono, H.; Masuda, H. *Inorg. Chem.* **1991**, *30*, 2610–2614.

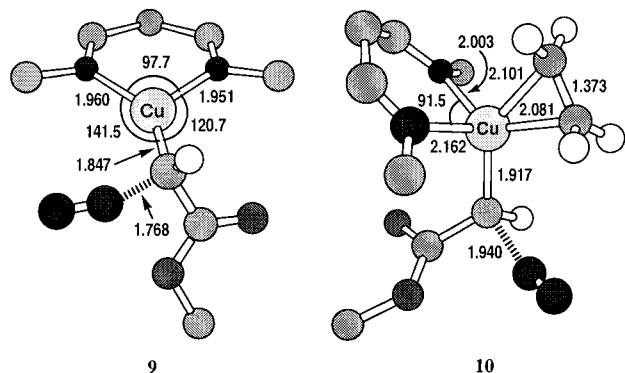
(41) Straub, B. F.; Rominger, F.; Hofmann, P. *Organometallics* **2000**, *19*, 4305–4309.

(42) (a) Willert-Porada, M. A.; Burton, D. J.; Baenziger, N. C. *J. Chem. Soc., Chem. Commun.* **1989**, 1633–1634. (b) Naumann, D.; Roy, T.; Tebbe, K.-F.; Crump, W. *Angew. Chem., Int. Ed. Engl.* **1993**, *32*, 1482–1483. (c) Eujen, R.; Hoge, B.; Brauer, D. J. *J. Organomet. Chem.* **1996**, *519*, 7–20.

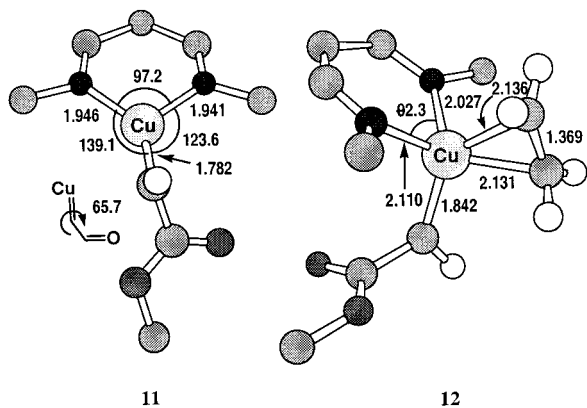
(43) Pearson, R. G. *J. Am. Chem. Soc.* **1963**, *85*, 3533–3539.

(44) Langford, C. H.; Gray, H. B. *Ligand Substitution Processes*; W. A. Benjamin: New York, 1965.

(45) (a) Cattalini, L.; Ugo, R.; Orio, A. *J. Am. Chem. Soc.* **1968**, *90*, 4800–4803. (b) Canovese, L.; Cattalini, L.; Uguagliati, P.; Tobe, M. L. *J. Chem. Soc., Dalton Trans.* **1990**, 3271–3276. (c) Johnson, L. K.; Killian, C. M.; Brookhart, M. *J. Am. Chem. Soc.* **1995**, *117*, 6414–6415. (d) Musaeov, D. G.; Froese, R. D. J.; Svensson, M.; Morokuma, K. *J. Am. Chem. Soc.* **1997**, *119*, 367–374. (e) Mikola, M.; Klika, K. D.; Hakala, A.; Arpalhti, J. *Inorg. Chem.* **1999**, *38*, 571–578.



**Figure 5.** Nonassisted (**9**) and olefin-assisted (**10**) transition structures for  $N_2$  extrusion (some hydrogen atoms have been omitted for clarity).



**Figure 6.** Nonassisted (**11**) and olefin-assisted (**12**) structures of the catalyst-carbene complex for the achiral reaction model (some hydrogen atoms have been omitted for clarity).

data on cyclopropanation reactions catalyzed by coordinated copper cations.<sup>46</sup>

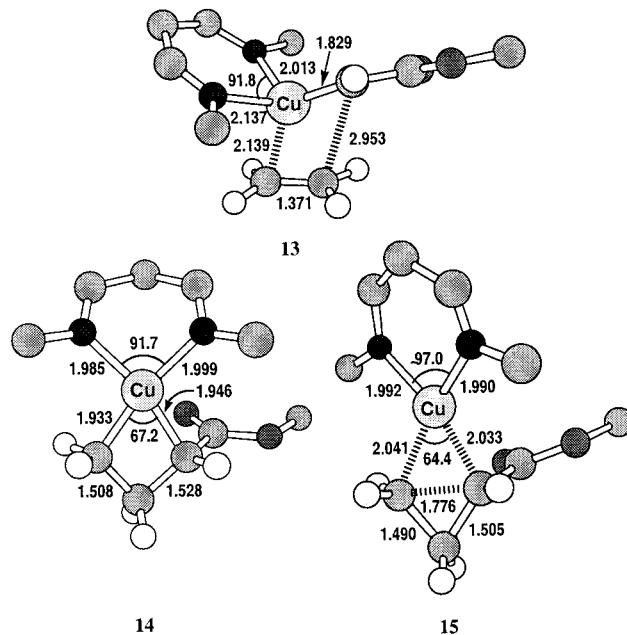
The structure of the catalyst-carbene complex (**11**) is shown in Figure 6. The copper-carbon bond has a length of 1.782 Å, slightly shorter than the value obtained from experimental data for other copper-carbene complexes (1.868–1.888 Å).<sup>47</sup> It can be seen that the carbonyl group adopts an almost perpendicular orientation (dihedral angle of 65.7°) with respect to the copper-carbon link, and this indicates a lack of conjugation between the two multiple bonds. This result is in accordance with experimental data for carbonylcarbene complexes of ruthenium.<sup>48</sup>

On the other hand, a noticeable difference between the two C-Cu-N bond angles (139.1° and 123.6°) is found, indicating that the copper-carbenoid carbon bond deviates significantly from the symmetry axis of the naked catalyst. This effect induces a noticeable approximation of the carbomethoxy substituent to one of the two methyl groups. This fact has significant consequences in terms of the stereochemical course of the reaction and this aspect will be discussed in more detail below. Although different conformations could, in principle, be considered for the catalyst-carbene complex depending on the relative orientation of carbomethoxy group in relation to the closer methyl substituent, only that shown in Figure 6 corresponds to an energy minimum.

(46) Anciaux, A. J.; Hubert, A. J.; Noels, A. F.; Petiniot, N.; Teyssé, P. *J. Org. Chem.* **1980**, *45*, 695–702.

(47) Raubenheimer, H. G.; Cronje, S.; Olivier, P. J. *J. Chem. Soc., Dalton Trans.* **1995**, 313–316.

(48) (a) Nishiyama, H.; Aoki, K.; Itoh, H.; Iwamura, T.; Sakata, N.; Kurihara, O.; Motoyama, Y. *Chem. Lett.* **1996**, 1071–1072. (b) Galardon, E.; Le Maux, P.; Toupet, L.; Simonneaux, G. *Organometallics* **1998**, *17*, 565–569.



**Figure 7.** Structures involved in the stepwise mechanism of cyclopropanation (**13**–**15**) (some hydrogen atoms have been omitted for clarity).

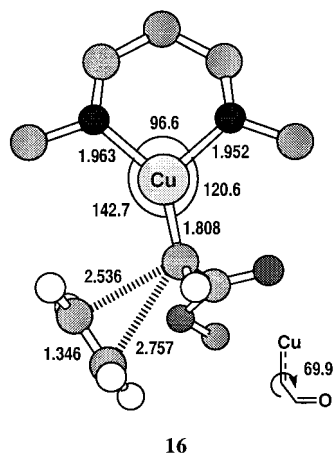
Our calculations indicate that the formation of the copper-carbene complex is favored from a thermodynamical viewpoint in both the elementary step ( $-14.3$  kcal mol<sup>-1</sup>) and the overall process in the reaction conditions ( $-1.0$  kcal mol<sup>-1</sup>).

It is known that olefins can bind to a number of transition metal-carbene complexes<sup>49</sup> and this leads to coordination compounds that can yield cyclopropanes by decomposition.<sup>50</sup> To gain an insight into the role of such species in the copper-catalyzed cyclopropanation reactions, an ethylene-catalyst-carbene complex (**12**) was considered, as shown in Figure 6. The coordination of the olefin to the catalyst-carbene complex is only slightly favored in terms of enthalpy ( $-4.0$  kcal mol<sup>-1</sup>), whereas it is clearly disfavored when free energies are considered (by 5.7 kcal mol<sup>-1</sup>).

**Formation of the Cyclopropane Product.** In the two-step pathway for the formation of cyclopropane, the carbene complex reacts with the olefin through an oxidative coupling to form a metallacyclobutane, which decomposes in an eliminative reduction to yield the reaction product. The key structures for this process are shown in Figure 7. Two different conformations are possible for the transition structure of the first step (denoted as **13**), depending on the relative disposition of the carbonyl group and the copper-carbon bond, with the *s-cis* form being favored. The lengths of the incipient bonds (2.139 Å for the copper-carbon interaction and 2.953 Å for the carbon-carbon link) indicate a large asynchronicity, with the creation of the C-C bond lagging behind the metal-carbon link. This result

(49) (a) Priester, W.; Rosenblum, M. *J. Chem. Soc., Chem. Commun.* **1978**, 26–27. (b) Schultz, A. J.; Brown, R. K.; Williams, J. M.; Schrock, R. R. *J. Am. Chem. Soc.* **1981**, *103*, 169–176. (c) Alvarez Toledano, C.; Levisalles, J.; Rudler, M.; Rudler, H.; Daran, J.-C.; Jeannin, Y. *J. Organomet. Chem.* **1982**, *228*, C7–11. (d) McGeary, M. J.; Tonker, T. L.; Templeton, J. L. *Organometallics* **1985**, *4*, 2102–2106. (e) Gabor, B.; Krüger, C.; Marczinke, B.; Mynott, R.; Wilke, G. *Angew. Chem., Int. Ed. Engl.* **1991**, *30*, 1666–1668.

(50) (a) Casey, C. P.; Vollendorf, N. W.; Haller, K. J. *J. Am. Chem. Soc.* **1984**, *106*, 3754–3764. (b) Alvarez Toledano, C.; Rudler, H.; Daran, J.-C.; Jeannin, Y. *J. Chem. Soc., Chem. Commun.* **1984**, 574–576. (c) Casey, C. P.; Shusterman, A. *J. Organometallics* **1985**, *4*, 736–744. (d) Casey, C. P.; Hornung, N. L.; Kosar, W. P. *J. Am. Chem. Soc.* **1987**, *109*, 4908–4916.



**Figure 8.** Transition structure for the direct carbene insertion (**16**) (some hydrogen atoms have been omitted for clarity).

agrees with theoretical data on analogous reactions of molybdenum derivatives.<sup>51</sup> A moderate activation barrier is found for the oxidative coupling (12.8 kcal mol<sup>-1</sup>).

The metallacyclobutane (**14**) presents a four-membered ring that is approximately coplanar with the ligand framework, in agreement with the square-planar coordination found in other copper(III) organometallic compounds,<sup>42</sup> and in contrast with the tetrahedral copper coordination proposed for analogous cyclopropanation intermediates.<sup>8,24d</sup> The lengths of the copper-carbon bonds are 1.933 and 1.946 Å, again in agreement with the experimental data for compounds such as other copper(III) organometallic compounds (1.863–2.026 Å)<sup>42</sup> or nickel(II) cyclobutanes (1.863–2.075 Å),<sup>52</sup> which are isoelectronic to the copper(III) analogues.

Two possible conformations for the transition structures of the eliminative reduction of the metallacyclobutane are possible (denoted as **15**). Calculations indicate a rather low activation barrier for this elementary step (2.3 kcal mol<sup>-1</sup>).

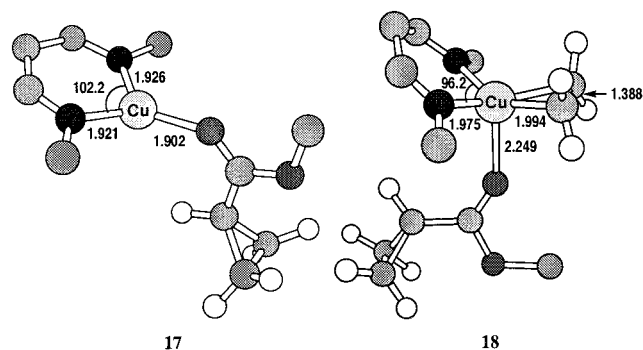
Two alternative conformations are possible for the transition structure of the direct carbene insertion (denoted as **16**) and these depend on the orientation of the carbonyl group relative to the attacking ethylene. The most stable form is shown in Figure 8. The ethylene approach takes place along the plane of the catalyst framework. The lengths of the incipient bonds (2.536 and 2.757 Å) indicate a very early transition structure, in a similar way to the Simmons–Smith cyclopropanation reactions.<sup>25</sup>

Interestingly, electronic energy data lead to a negative activation barrier (–2.5 kcal mol<sup>-1</sup>). This anomalous result can be attributed, at least partially, to the neglect of solvent and counterion effects in this work, leading thus to an exaggerated stabilization of the interaction between neutral ethylene and the cationic catalyst.

The stability of transition states in association processes is decreased when entropy effects are considered. Thus, Gibbs free energy data indicate a moderate positive activation barrier (9.8 kcal mol<sup>-1</sup>) for the direct carbene insertion. Thus, this mechanism is favored over the stepwise pathway by 3 kcal mol<sup>-1</sup>. Furthermore, the high reactivity of the copper-carbene complex explains the lack of experimental evidence for its formation under cyclopropanation reaction conditions.

The possibility of olefin-assisted pathways for both two-step and direct mechanisms for the cyclopropanation reaction was also considered. However, transition structures could not be localized even after an extensive search. It can therefore be

(51) Wu, Y.-D.; Peng, Z.-H. *J. Am. Chem. Soc.* **1997**, *119*, 8043–8049.



**Figure 9.** Nonassisted (**17**) and olefin-assisted (**18**) catalyst-product complexes (some hydrogen atoms have been omitted for clarity).

concluded that only the nonassisted mechanisms are possible for the copper-catalyzed cyclopropanation.

Both direct carbene insertion and stepwise pathways yield a catalyst-product complex (**17**, Figure 9). The regeneration of the starting catalyst requires the coordination of an ethylene molecule and the departure of the product. Two alternative pathways can be considered according to the timing of these processes and these are called dissociative and associative displacements. The dissociative mechanism involves the decoordination of the reaction product to yield the naked catalyst, which subsequently coordinates an ethylene molecule. The decoordination of the product involves a high energy rise (26.2 kcal mol<sup>-1</sup>).

However, the associative pathway through an ethylene-catalyst-product complex (**18**) is greatly favored. An approximately tetrahedral coordination is found for copper.

Calculations indicate that ethylene coordination is clearly favored (by –12.3 kcal mol<sup>-1</sup>). Surprisingly, the regeneration of the starting catalyst requires an energy of 4.3 kcal mol<sup>-1</sup>. This result contrasts with the lack of experimental data indicating product inhibition. However, the influence of the product coordination has been shown to be important in one example of a product-accelerated reaction.<sup>53</sup> This situation is too complex to be explained by the relatively simple model considered in this work. The influence of several factors (such as solvent, counterion, byproducts with coordination ability such as fumaric and maleic esters, or the participation of a second molecule of ligand) may have an influence on the regeneration of the catalytic species. The reaction product is methyl cyclopropane carboxylate (**19**).

Free energy results indicate that the overall process is largely favored from a thermodynamical viewpoint (–51.9 kcal mol<sup>-1</sup>). The large magnitude of this value agrees with the irreversible character of the cyclopropanation reactions.

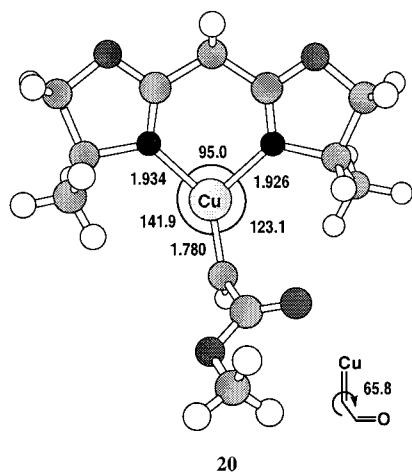
**Extension to Chiral Models.** The results obtained with the nonchiral diimine–Cu(I) model give valuable information about the general mechanism of the copper(I)-catalyzed cyclopropanation reactions, including some insights into the origin of the stereoselectivity. However, the simplicity of the model precludes a detailed discussion on the origin of either the enantioselectivity or the *cis/trans* selectivity.

To cover these points with greater certainty, some other models were considered that resembled more closely the systems used experimentally. As the chiral ligand we chose a simplified

(52) (a) Hughes, R. P.; Carl, R. T.; Samkoff, D. E.; Davis, R. E.; Holland, K. D. *Organometallics* **1986**, *5*, 1053–1055. (b) Krüger, C.; Laakmann, K.; Schroth, G.; Schwager, H.; Wilke, G. *Chem. Ber.* **1987**, *120*, 471–475.

(53) Adrián, F.; Burguete, M. I.; Fraile, J. M.; García, J. I.; García, J.; García-España, E.; Luis, S. V.; Mayoral, J. A.; Royo, A. J.; Sánchez, M. C. *Eur. J. Inorg. Chem.* **1999**, 2347–2354.





**Figure 10.** Catalyst-carbene complex for the chiral reaction model (**20**).

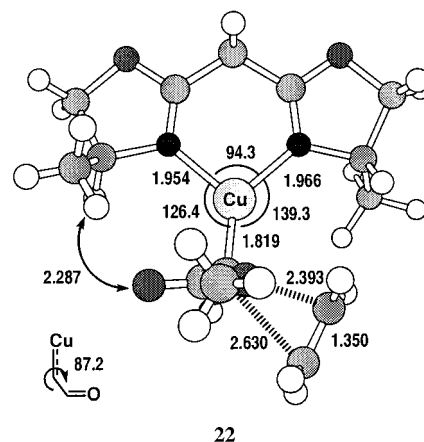
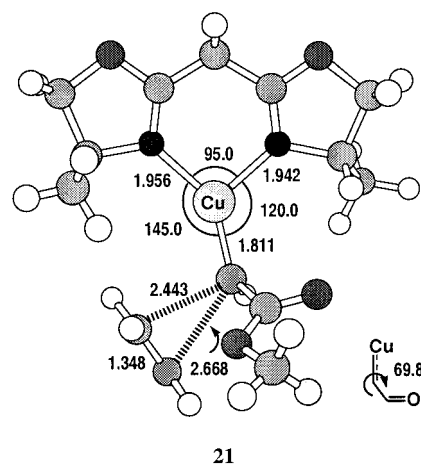
bis(oxazoline) structure, namely 2,2'-methylenebis[(4*S*)-methyl-2-oxazoline]. The corresponding Cu(I)-carbene complex (**20**) was calculated at the B3LYP/6-31G(d) theoretical level, and the resulting lowest energy structure is shown in Figure 10.

The structural parameters of the bis(oxazoline)-Cu(I)-carbene complex (**20**) are very similar to those calculated for the nonchiral model **11**. The main structural features—namely the axial deviation of the copper-carbenoid carbon bond and the twisted disposition of the ester group with regard to the copper-carbon bond—are also present in complex **20** and the bond lengths and angles are very close to those calculated for complex **11**.

The transition structures corresponding to the direct carbene insertion into the double bond of the ethylene molecule were located and properly characterized. Given the presence of a chiral ligand, there are two possible diastereomeric transition structures that arise from the approach of the olefin molecule to the two alternative *Re* (**21**) and *Si* (**22**) faces of the plane defined by the Cu=C-C arrangement. Each approach leads to different configurations at C1 of the cyclopropane ring. The two transition structures are shown in Figure 11 and Figure S1 (Supporting Information).

From the structural viewpoint, both TS correspond to a concerted and asynchronous reaction path, and both are somewhat later than **16**, as indicated by the shorter carbon-carbon bond forming distances. The rest of the geometrical features of the two TS are otherwise very similar. In the case of TS **22**, a short distance (2.287 Å) is found between the carbonyl oxygen atom and one of the hydrogen atoms of the bis(oxazoline). This steric interaction is partially relieved by opening the N-Cu-C bond angle (from 120.0° in **21** to 126.4° in **22**), lengthening the Cu-N bonds (from 1.942 and 1.956 in **21** to 1.954 and 1.966 in **22**), and twisting the ester group with regard to the Cu-C bond (from 69.8° to 87.2° on changing from **21** to **22**).

The calculated free energies of activation are 11.5 and 14.1 kcal mol<sup>-1</sup> for **21** and **22**, respectively, which are slightly higher than the corresponding activation barrier calculated for the nonchiral model (9.8 kcal mol<sup>-1</sup>). As far as the enantioselectivity is concerned, TS **21** is favored over **22** by 2.6 kcal mol<sup>-1</sup>. These results are in qualitative agreement with the stereochemistry of the major products obtained experimentally in the reaction of styrene with ethyl diazoacetate, catalyzed by related 2,2'-isopropylidenebis[(4*S*)-alkyl-2-oxazolines].<sup>10-12</sup> To obtain more reliable energy values, single-point energy calculations were carried out at the B3LYP/6-311+G(2d,p) level using the



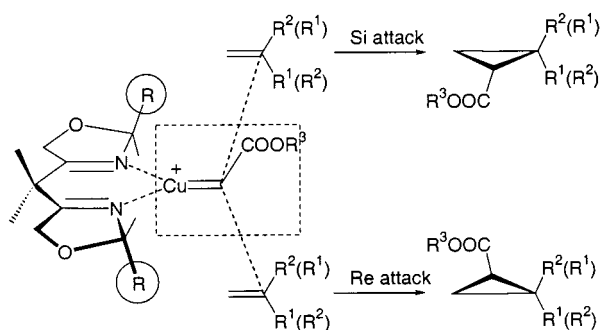
**Figure 11.** Transition structures of the cyclopropanation step for the ethylene attack to *Re* (**21**) and *Si* (**22**) faces of the chiral catalyst-carbene complex.

B3LYP/6-31G(d) geometries. By using the zero-point energy and thermal corrections calculated at the B3LYP/6-31G(d) level, the energy difference between the two TS drops to 1.9 kcal mol<sup>-1</sup>. This value, although still large, is closer to that expected for a chiral ligand with low stereodiscrimination.

Solvent effects were also considered by means of continuum model calculations. On passing from a vacuum to a dichloromethane solution, the free energy activation barriers change to 13.3 and 15.3 kcal mol<sup>-1</sup>, i.e. a slight increase in the activation barriers is caused by solvation. This is undoubtedly due to the greater solvation energy of the carbene complex **20** in comparison to the TS, in which the positive charge is more delocalized. From the enantioselectivity viewpoint, it can be seen that **22** is slightly more solvated than **21** (by 0.6 kcal mol<sup>-1</sup>). Thus, by combining the single-point energy, frequency, and solvation energy calculations, we estimate an energy difference between **21** and **22** of only 1.3 kcal mol<sup>-1</sup>. This result is in better agreement with the experimental values found for related systems.<sup>10-12</sup>

The structural and energy data for these transition structures allow us to propose an asymmetric induction model for the cyclopropanation reaction (Scheme 3), which has many common points with that formulated by Pfaltz.<sup>4,16</sup> It must be emphasized, however, that the latter model was not based on any direct experimental or theoretical evidence, but only on the assumption of a direct carbene insertion. In contrast, other authors have explained the stereoselectivity of the reactions by assuming a two-step mechanism, although in these cases there is also a lack of direct evidence.<sup>8,24</sup>



**Scheme 3.** Asymmetric Induction Model for Enantioselective Cu Complex Catalysts


The reaction model allows us to account for the major enantiomers found in the cyclopropanation reactions catalyzed by common Cu(I) catalysts. The high face-discriminating ability of the substituents situated on the chelate structure is attributed to the steric repulsion with the alkoxy-carbenoid group in the transition state. An interpretation of this interaction was described by Pfaltz in terms of an advanced degree of pyramidalization of the carbenoid carbon in the transition state.<sup>4</sup> However, given the reactant-like nature of the transition structure, this proposal cannot totally account for the high enantioselectivities usually found in this kind of reaction. Instead, our results indicate that the noticeable interaction between the alkoxy-carbenoid group and the chelate substituent is essentially due to the deviation of the copper–carbenoid carbon bond relative to the symmetry axis of the naked catalyst.

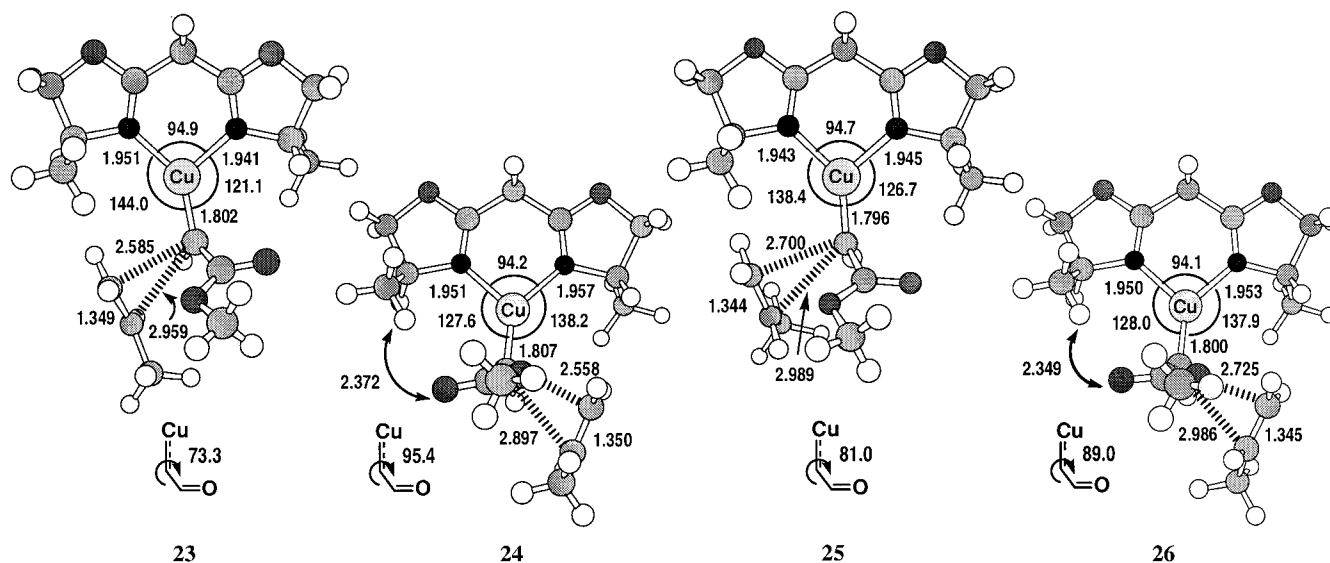
The absolute configuration of C2 and, as a consequence, the *cis* vs *trans* stereochemistry of the cycle are determined in each case by the mutual steric repulsion between the alkoxy-carbenoid group and the substituents bonded to the prochiral carbon of the olefin. This kind of selectivity clearly cannot be studied with the precedent chiral model because of the absence of substituents on the ethylene molecule. To investigate the *cis/trans* selectivity, we considered a somewhat more complex model in which ethylene was replaced by propene. In principle, the consideration of a substituted double bond leads to eight possible transition structures. However, due to steric interactions with the chiral ligand, it is reasonable to suppose that the approach of the propene molecule will always occur with the

methyl group far away from the bis(oxazoline). This assumption reduces the possibilities to four, namely the *Re-cis*, the *Si-cis*, the *Re-trans*, and the *Si-trans*, represented in Scheme 3. The corresponding transition structures are denoted as **23–26**, respectively.

All of the transition structures apart from *Re-trans* (**25**) could be located and properly characterized at the B3LYP/6-31G(d) theoretical level. Some of the structural features of these TS are shown in Figure 12 and Figure S2 (Supporting Information). In the case of TS **25**, none of the strategies used to converge to a transition structure resulted in success. The most probable explanation for this result is the extremely flat potential energy surface (PES) around this stationary point, resulting from the greater reactivity of propene in comparison to ethylene (see below). However, an extensive computational search allowed us to locate a structure that, though not properly converged since the small eigenvalues of the Hessian matrix lead to high displacement values, has essentially zero forces, and is in the correct curvature zone of the PES (one and only one imaginary frequency, corresponding to the C–C bond formation). Following the suggestion of one referee, we include the structure and energy of this structure (**25**) for the sake of a more clear explanation. In the other three cases (**23**, **24**, and **26**), the steric interactions, either intra- or intermolecular, result in a more clearly defined maximum energy in the direction of the reaction coordinate, and hence to an easier convergence to a transition structure.

From the structural viewpoint, the three located TS and structure **25** show great similarities with **21** and **22**. The most marked differences are found in the longer carbon–carbon bond forming distances, which indicate the more pronounced steric effect of propene over ethylene. The “*cis*” TS (**23** and **24**) show a greater asynchronicity with regard to the “*trans*” TS (**25** and **26**) and to the TS of the ethylene reaction (**21** and **22**) ( $\Delta d_{C-C} = 0.374$  and  $0.339$  Å against  $0.289$ ,  $0.261$ ,  $0.225$ , and  $0.237$  Å, respectively), which clearly indicates steric repulsion between the methyl group of propene and the ester group of the carbene complex.

In the cases of the *Re* attack of the propene (**24** and **26**), there are clear steric interactions between the carbonyl oxygen atom and one of the hydrogen atoms of the bis(oxazoline) ligand. As in the case of ethylene, this steric interaction is partially



**Figure 12.** Transition structures of the cyclopropanation step for the propene attack to the catalyst–carbene complex through the *Re-cis* (**23**), *Si-cis* (**24**), *Re-trans* (**25**), and *Si-trans* (**26**) approaches.

relieved by opening the N–Cu–C bond angle and, above all, twisting the ester group with respect to the Cu–C bond (Figure 12).

As a referee noted, there is a connection between the origin of the enantioselectivity in these systems and the mechanism of stereoselectivity in the olefin polymerization, catalyzed by  $C_2$ -symmetric group IV metallocenes.<sup>54</sup> In both cases, the steric interaction of the metal-coordinated reactive with the chiral ligand is determinant for the stereochemistry of the products.

The calculated free energies of activation for **23**, **24**, **25** (estimated), and **26** at the B3LYP/6-31G(d) level are 10.5, 12.4, 9.8, and 11.0 kcal mol<sup>-1</sup>, respectively. These values indicate that propene is more reactive than ethylene for the carbene insertion, as one would expect on the basis of electronic considerations. In this case, the single-point B3LYP/6-311+G-(2d,p) energy values do not significantly alter the relative stability of the TS, and the corresponding free energy barriers change to 10.6, 12.1, 10.0, and 11.1 kcal mol<sup>-1</sup>, respectively. The inclusion of the solvation energy, calculated at the IPCM B3LYP/6-31G(d) level, changes the activation barriers to 12.5, 13.4, 11.3, and 12.2 kcal mol<sup>-1</sup>, respectively. Therefore, it can be seen that the relative energy ordering of the different transition structures is in perfect qualitative agreement with the stereochemistry of the cyclopropane products obtained experimentally in the copper-catalyzed reactions of styrene with ethyl diazoacetate, using related bis(oxazoline) ligands.<sup>10–12</sup> By comparing the energies of **23** and **25**, or **24** and **26**, we can estimate the *cis/trans* selectivity. The combination of B3LYP/6-311+G(2d,p) single-point energies, B3LYP/6-31G(d) zero-point and thermal energy corrections, and solvation energies (in dichloromethane) leads to an energy difference between the two TS of 1.2 kcal mol<sup>-1</sup>. This value is in satisfactory agreement with the 0.5–0.7 kcal mol<sup>-1</sup> obtained for the reactions catalyzed by the 2,2'-isopropylidenebis[(4*S*)-alkyl-2-oxazoline]–Cu(I) complexes.<sup>10–12</sup>

Comparison of the energies of **23** and **24** or **25** and **26** leads to an estimate of the enantioselectivity in the *cis* and *trans* cyclopropanes, respectively. The combination of B3LYP/6-311+G(2d,p) single-point energies, B3LYP/6-31G(d) zero-point and thermal energy corrections, and solvation energies (in dichloromethane) gives an energy difference between the two TS of 1.1 and 0.9 kcal mol<sup>-1</sup>, for the *cis* and *trans* couples, respectively. These values appear very reasonable when compared with the 1.7 kcal mol<sup>-1</sup> obtained for the reaction of styrene with ethyl diazoacetate catalyzed by the 2,2'-isopropylidenebis-[(4*S*)-*tert*-butyl-2-oxazoline]–Cu(I) complex,<sup>12</sup> which contains a much more stereodiscriminating chiral ligand.

Therefore, the results obtained with these models confirm the origin of the stereoselectivity proposed in the Pfaltz model, and provide a solid basis to investigate related catalytic systems. In particular, they will help to perform hybrid QM/MM calculations on models which include most of the structural features of the real catalytic systems. These kinds of calculations are ongoing and the results will be reported in due course.

## Conclusions

DFT calculations predict the existence of a reaction mechanism that is consistent with experimental data obtained for

related systems. Under the reaction conditions most of the catalyst is coordinated with one olefin molecule. Thus, the 1:1 catalyst–ethylene complex is considered as the starting species for a catalytic cycle. Ethylene can be replaced by the diazo ester through an associative displacement. The catalyst–diazo compound complex thus formed presents a metal–carbon bond, in agreement with the behavior of Cu(I) as a soft Lewis acid. This species can extrude nitrogen to yield a metal–carbene complex and this process is the rate-limiting step.

The copper atom of the carbene complex has a distorted trigonal coordination, the metal–carbon bond being moved away from the symmetry axis of the catalyst ligand. Calculations indicate that a direct carbene insertion is favored over a stepwise process in the step that controls the stereoselectivity.

The formation of the catalyst–product complex is greatly favored for the cyclopropanation step. The regeneration of the catalyst–ethylene complex takes place through an associative displacement. The endergonic step of decoordination of the cyclopropane product is probably due to the use of a simple system to model the experimental cyclopropanation reactions.

The possibility of dissociative mechanisms for the ligand exchange in two steps of the catalytic cycle has been considered, although calculations show that these pathways are clearly disfavored. The possibility of an olefin-assisted pathway has also been considered for the formation of the metal–carbene complex and the cyclopropanation steps, although calculations again indicate that these mechanisms are disfavored.

The origin of the stereoselectivity in the carbene insertion step has been investigated through DFT calculations on chiral bis(oxazoline)–Cu(I) system models. The steric interaction between the ester group and one of the substituents of the bis(oxazoline) ligand is in the origin of the enantioselectivity. This steric interaction is enhanced by the axial deviation of the Cu=C carbene bond with regard to the complex. On the other hand, the *cis/trans* selectivity in the final cyclopropanes is governed by the steric interaction between the carbene ester group and the substituents on the olefinic double bond.

In summary, a thorough examination of the free energy surface of the model reaction studied has allowed the elucidation of the key steps in the mechanism of copper-catalyzed cyclopropanation reactions. This information provides new insights into the origin of the stereoselectivities observed, which should allow the design of more efficient catalytic systems.

**Acknowledgment.** Dedicated to Prof. José Elguero on the occasion of his Doctorate “Honoris Causa” from the University of Zaragoza. This work was made possible by the generous financial support of the Comisión Interministerial de Ciencia y Tecnología (Project MAT99-1176).

**Supporting Information Available:** Tables of electronic energies, as well as enthalpies, entropies, Gibbs free energies (the last three data series at 25 °C), and the lowest frequencies for the different conformations of the structures considered in this work and figures of transition states **21–26**, projected along the Cu=C bond (PDF). This material is available free of charge via the Internet at <http://pubs.acs.org>. Geometries of the structures discussed in this paper are available upon request from the authors.

(54) (a) Resconi, L.; Cavallo, L.; Fait, A.; Piemontesi, F. *Chem. Rev.* **2000**, *100*, 1253–1345. (b) Angermund, K.; Fink, G.; Jensen, V. R.; Kleinschmidt, R. *Chem. Rev.* **2000**, *100*, 1457–1470.